

Low Complexity Decoding for Punctured Trellis-Coded Modulation Over Intersymbol Interference Channels

Fabian Schuh and Johannes B. Huber

Institute for Information Transmission, Friedrich-Alexander-Universität Erlangen-Nürnberg, Germany

mail: {schuh, huber}@LNT.de

Abstract—Classical trellis-coded modulation (TCM) as introduced by Ungerboeck in 1976/1983 uses a signal constellation of twice the cardinality compared to an uncoded transmission with one bit of redundancy per PAM symbol, *i.e.*, application of codes with rates $\frac{n-1}{n}$ when 2^n denotes the cardinality of the signal constellation. The original approach therefore only comprises integer transmission rates, *i.e.*, $R = \{2, 3, 4 \dots\}$, additionally, when transmitting over an intersymbol interference (ISI) channel an optimum decoding scheme would perform equalization and decoding of the channel code jointly.

In this paper, we allow rate adjustment for TCM by means of puncturing the convolutional code (CC) on which a TCM scheme is based on. In this case a nontrivial mapping of the output symbols of the CC to signal points results in a time-variant trellis. We propose an efficient technique to integrate an ISI-channel into this trellis and show that the computational complexity can be significantly reduced by means of a reduced state sequence estimation (RSSE) algorithm for time-variant trellises.

Index Terms—trellis-coded modulation (TCM); punctured convolutional codes; Viterbi-Algorithm (VA); ISI-channel;

I. INTRODUCTION

Ungerboeck's trellis-coded modulation (TCM) [1] is a bandwidth efficient digital transmission scheme when very low overall latency is desired. Low latency is ensured by the use of convolutional codes instead of block codes (*cf.* [2]) and the dispense with interleaving (as opposed to conventional bit-interleaved coded modulation [3]).

Ungerboeck showed that a significant increase in the Asymptotic Coding Gain (ACG) can be achieved when considering channel coding and modulation jointly. By expanding the constellation from 2^{n-1} to 2^n signal points and employing a rate- $\frac{n-1}{n}$ convolutional encoder one can improve the robustness of the transmission against noise by up to 6 dB without any further costs besides some computational effort. However, TCM is strictly limited to integer transmission rates.

Our approach applies *punctured* TCM (P-TCM) with an arbitrary rate. We extend P-TCM to intersymbol interference (ISI)-channel scenarios. In this case, ML-decoding can be performed by efficiently incorporating the ISI-channel into the trellis.

We show that reduced-state sequence estimation (RSSE) can be applied in order to reduce computational complexity. We were able to show in [4], [5] that for minimum phase channels, the number of states to decode must *not* be significantly higher than the number of states in the channel encoder. In this paper we will describe the application of RSSE to P-TCM

and discuss the partitioning of the time-variant trellis into hyperstates.

This paper is structured as follows: In Sec. II we first introduce notation and present the system model. Sec. III briefly recapitulates a presentation technique that enables the implementation of punctured encoding. The application of RSSE for P-TCM is given in Sec. IV. Final results of numerical simulation and conclusions are given in Sec. V and Sec. VI, respectively.

II. SYSTEM MODEL

This paper deals with convolutionally encoded pulse-amplitude modulated (PAM) transmission as depicted in Fig. 1. (Here, the term PAM is used for complex-valued signal constellations \mathcal{A} as well including amplitude-shift keying (ASK), phase-shift keying (PSK) or quadrature-amplitude modulation (QAM).) A binary data sequence $\langle u \rangle$ is encoded using a rate-

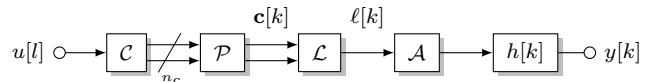


Fig. 1. Concatenation of a rate- $\frac{1}{2}$ convolutional encoder \mathcal{C} and puncturing \mathcal{P} with labeling and modulation ($n_u = 0$, $n_c = 2$).

rate- $\frac{n_c-1}{n_c}$ binary convolutional encoder \mathcal{C} with generator polynomials $g_{ij}(D)$, $1 \leq i \leq n_c$; $1 \leq j \leq n_c - 1$, with delay operator D , $n_c - 1$ parallel binary-input symbols and n_c parallel output symbols at each time instant.

At each output of the encoder, the symbols traverse through a puncturing system with puncturing matrix $\mathbf{P} = [P_{ij}]$, $P_{ij} \in \{0, 1\}$; $1 < i \leq n_c$; $1 < j < \Omega$ and period Ω . For each (n_c) -tuple of encoder output symbols the puncturing scheme cyclically advances by one step. Where P_{ij} is zero, the current symbol at the output is discarded, accordingly.

The punctured encoded output symbols $c[k]$ are labeled to $\ell[k]$ before being mapped to the $M = 2^{n_u+n_c} = 2^n$ -ary signal constellation \mathcal{A} .

The modulated (possibly complex-valued) transmit signal traverses through a memory- L discrete-time ISI-channel with $L + 1$ channel coefficients $h[k]$ with k denoting the discrete time index.

The task of the receiver is to estimate for the information bits given the transmit signal $y[k]$ plus additive noise. Here, we focus on perfect channel knowledge at the receiver-side.

III. PUNCTURED TRELLIS-CODED MODULATION

In the following, we will briefly recapitulate punctured convolutional trellis coded transmission over ISI-channel scenarios as introduced in [5].

In contrast to classical TCM, our approach using *punctured* convolutional codes results in nontrivial mapping of coded bits to modulation symbols. As a consequence, the trellis is time-variant as already described in [5]–[7].

In order to briefly recapitulate decoding concept for punctured trellis coded modulation, we focus on 4-ary ASK-modulation, a memory-2 convolutional code, and a short puncturing scheme namely $\mathbf{P} = [(11)^T (01)^T]$. Note that, whenever the number of erased bits in one period of the puncturing scheme is not dividable by $\log_2(M)$, the puncturing scheme has to be repeated until this condition is fulfilled. This restriction ensures that entire modulation symbols can be constructed by the finite state machine (FSM). In our example, the puncturing period (e.g., $[(11)^T (01)^T]$) has to be applied twice. As can be seen from the encoding process in Fig. 2, the third and the seventh encoded symbol are punctured and do not contribute to the labeling and modulation process. Thus, the second symbol, i.e., $a[k+1]$, contains information about $u[l+1]$ and $u[l+2]$ and the third symbol, i.e., $a[k+2]$, contains information about $u[l+2]$ and $u[l+3]$.

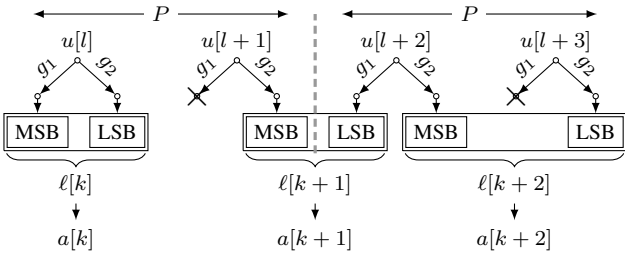


Fig. 2. Encoding process for a rate- $\frac{2}{3}$ punctured convolutional code and natural labeling. Overall transmission rate $R = \frac{4}{3}$.

When decoding the second symbol (e.g., $a[k+1]$), a decision can be made for $u[l+1]$ but not for $u[l+2]$, as a portion of information will be received in the consecutive symbol. Thus, the trellis has to be expanded in order to use the symbols $a[k+1]$ and $a[k+2]$ when decoding $u[l+2]$. As sample trellis is given in Fig. 3.

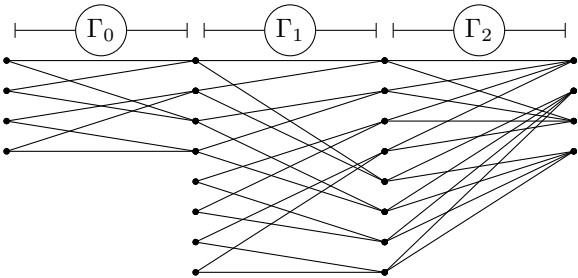


Fig. 3. Time-variant trellis for a punctured rate- $\frac{2}{3}$ convolutional code. In the first to VA steps, two transitions arrive at each state, i.e., one bit can be estimate, whereas the third step allows an estimation for two bits.

To algorithmically handle the time-variant mapping we introduced a set of so-called generator offsets \mathcal{T}_i which describe, depending on the puncturing scheme, modulation size, and time instant, the relations between generator polynomials, input value, FSM state, and mapping to MSB or LSB, respectively. For each new generator offset \mathcal{T}_i a new trellis segment

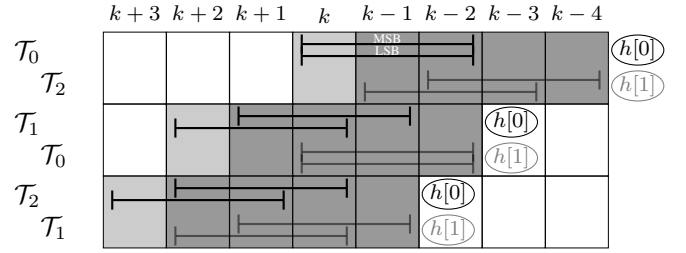


Fig. 4. State transitions of the transmitter FSM with $R = 4/3$ and the relations between generator polynomials, FSM-state/input and channel state for a memory-1 ISI-channel.

arises, e.g., the number of generator offsets equals the number of trellis segments in one trellis period.

When transmitting over an ISI-channel, several symbols are stored in the memory of the ISI-channel independently from the encoding and puncturing process. Thus, multiple generator offsets \mathcal{T}_i have to be considered simultaneously. This can be seen from Fig. 4 for a memory-1 channel. There, the resulting sequence of used generator offsets is depicted. This scheme can easily be extended to arbitrary lengths of the ISI-channel. A detailed description as well as an algorithm to construct such trellises will be given in a separate full-length paper.

IV. REDUCED-STATE SEQUENCE ESTIMATION

Reduced-state sequence estimation (RSSE) [8] is proposed to reduce the number of states at the cost of small loss in Euclidean distance. In order to introduce RSSE for P-TCM, we first briefly recapitulate *delayed decision-feedback sequence estimation* (DFSE) [9].

A. Delayed Decision Feedback Sequence Estimation

When equalizing (uncoded) digital PAM signaling over a discrete-time ISI-channel with $L+1$ taps using DFSE (i.e., no decoding), the trellis is constructed from the first $\tilde{L} \leq L$ taps only. Thus, the number of states is reduced from M^L to $M^{\tilde{L}}$.

The remaining $L+1-\tilde{L}$ channel taps are considered in a delayed decision-feedback equalization (DFE) that is performed in each trellis state using the *delayed* path register of the corresponding state.

The main difference to full state equalization appears in the metric computation for each time instant. From (1) it becomes clear that the state specific path register $p_{\text{reg}}[k, \mathbf{s}]$ is delayed by \tilde{L} and its elements are multiplied by the subsequent channel coefficients $h_{\text{dfe}}[h]$ which have not been considered in the trellis. The branch metric $\lambda(\mathbf{s}, \mathbf{u})$ (e.g., Euclidean distance of the received symbol $y[k]$ to the hypotheses $h(\mathbf{s}, \mathbf{u})$ for the states \mathbf{s} and bits \mathbf{u}) thus includes the correction factor δ :

$$\delta = \sum_{\kappa} p_{\text{reg}}[k - \tilde{L} + \kappa, \mathbf{s}] \cdot h_{\text{dfe}}[\kappa] \quad (1)$$

$$\lambda(\mathbf{s}, \mathbf{u}) = |y[k] - h(\mathbf{s}, \mathbf{u}) - \delta|^2$$

B. Reduced State Sequence Estimation

For our coded transmission over ISI-channel we consider RSSE instead. Here, Z arbitrary MLSE states, each with $M = 2^K$ possible branches to adjacent states, are combined

into $Z_R = \frac{Z}{2^J}$; $J \in \mathbb{N}$ hyperstates [10] each having 2^J substates and $2^K \cdot 2^J$ branches. A certain assignment of states to hyperstates is called a *partitioning* [10].

Instead of having 2^K arriving branches at each of the Z MLSE states we get a set of $2^K \cdot 2^J$ branches at each of the Z_R hyperstates. The total number of available branches remains $2^K \cdot Z$. However, when using RSSE only 2^K branches are possible (*i.e.*, *enabled*) from each state, at a given time instant. The availability of branches is determined by the path registers, and thus form a decision-feedback.

The metric computation in this case can be implemented as depicted in Algorithm 1. Note that with line 6 only M branches are activated. Thus, the VA has to decide between M survivor branches at each state giving an estimate for $\log_2(M)$ bits.

Algorithm 1 Metric calculations for RSSE

```

1:  $\tilde{L} \leftarrow \log_2(\text{nr. hyperstates}) / \log_2(M)$ 
2:  $\ell \leftarrow \log_2(\text{nr. substates}) / \log_2(M)$ 
3: for all  $\mathbf{s} \in \mathcal{S}$  do
4:   for all  $\mathbf{u} \in \mathcal{A} \cdot K$  do
5:     for all  $\kappa = 1 \rightarrow \ell$  do
6:        $\zeta[\kappa] = p_{\text{reg}}(\text{end} - \tilde{L} + \kappa, \mathbf{s})$        $\triangleright$  active branches
7:     end for
8:      $\lambda(\mathbf{s}, \mathbf{u}) \leftarrow |y[k] - h(\zeta, \mathbf{u})|^2$        $\triangleright$  branch metric
9:      $\lambda(\mathbf{s}, \mathbf{u}) \leftarrow \lambda(\mathbf{s}, \mathbf{u}) + \Gamma(\mathbf{s})$        $\triangleright$  acc. path metric
10:   end for
11: end for

```

For time-variant trellises some modifications to the underlying VA are necessary, which are described in [5].

The main difference to MLSE is, that we decide for a surviving path prematurely resulting in a truncation of error events. A loss in Euclidean distance appears if an error event with minimum Euclidean distance gets truncated. Therefore the performance of RSSE strongly depends on the partitioning of the states into hyperstates. Instead of exhaustively search for the optimum state partitioning, which maximizes the intra-hyperstate distance [10], we exploit the minimum phase characteristics of the ISI-channel which is, as described above, fully integrated into our trellis.

For a minimum phase channel impulse response the prior channel input symbols are weighted less than more recent ones and, thus, affect the metric less. The elder the symbols, the further back it is stored in the vector presentation of a particular trellis state. Hence, the intra-hyperstate distance is maximized when states are combined with respect to elder positions in the state number. This particular partitioning is equivalent to DFSE for ISI-channels (which is the optimum partitioning for equalization of minimum phase ISI-channels [10]) and will in the latter be called *DFSE partitioning*. As the minimum phase ISI-channel is the last element to affect the transmitted symbols and is also fully integrated into the trellis, we can apply the *DFSE partitioning* to use RSSE for P-TCM over ISI-channels. An implementation of this set partitioning for the J^{th} level exploiting the minimum phase characteristics is shown in Algorithm 2. The columns in the resulting matrix $p(z, i)$ define the states that have to be grouped into hyperstates.

Algorithm 2 DFSE Partitioning for RSSE

```

1:  $i, z \leftarrow 1$ 
2: for  $\ell = 1 \rightarrow Z$  do
3:   if  $\ell \bmod J = 0$  then
4:      $z \leftarrow z + 1$ 
5:   end if
6:    $p(z, i) = \ell$ 
7:    $i \leftarrow i + 1$ 
8: end for

```

In the following we will focus on our state design and two possibilities to apply *DFSE partitioning* to time-variant trellises.

C. State Design

In Fig. 5 a single trellis state in the VA is depicted as a FIFO. Input values to the FSM are represented by the branches at the left-hand side, whereas values that drop of the FIFO are stored within the state-specific path register $p_{\text{reg}}(k, \mathbf{s})$ at the right-hand side. During decoding when entering a trellis

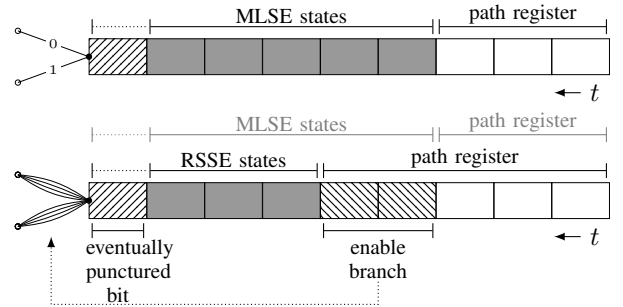


Fig. 5. Graphical representation of our state design for punctured convolutional coding with and without reduced-state sequence estimation.

segment that is split, *i.e.*, has an increased number of states, the two possibilities for the punctured bit are tracked using an additional delay element, indicated by the hatched block ⊘ .

When DFSE partitioning is performed, the states can be reduced as shown in Fig. 5. There, fewer FIFO elements are used to define the trellis state, while the remaining ones are used as feedback to enable branches for the next trellis step for that particular state.

An implementation of this algorithm needs to ensure that when entering a split trellis segment, *i.e.*, increased number of states, the right path register is chosen as source for the decision feedback.

D. State Partitioning

As already mentioned, a DFSE partitioning of the first order, *i.e.*, reducing the number of states in each trellis segment by a factor of two, combining states that differ in the eldest position, into hyperstates. Hence, when applied to a punctured TCM, each trellis segment undergoes the same partitioning. A resulting reduced-state trellis is depicted on the left-hand side of Fig. 6 for $J = 1$ and $J = 2$. As a consequence, non-existing states from the original trellis are also partitioned (*cf.*, first trellis segment).

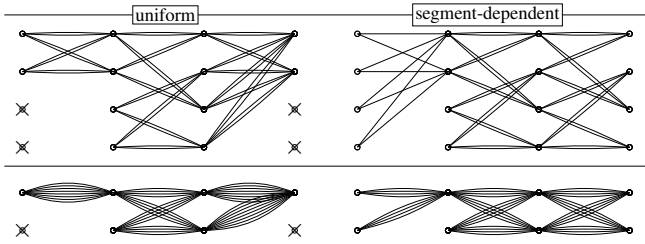


Fig. 6. Illustration of uniform and segment-dependent partitioning for $J = \{1, 2\}$.

Due to the reduction of non-existing states, and hence reduced minimum Euclidean distance, we propose to partition those segments first that are split and keeping the others unpartitioned. As can be seen from the first-level state reduction in Fig. 6 (right-hand side, above), the first segment contains two transitions in each state, and thus is not partitioned, whereas in segment two and three, each state has four transitions, due to the state partitioning.

Apparently, the first segment may be handled with a full state VA, while the other two segments need to be decoded via RSSE using the path register in each state.

The right-hand side of Fig. 6 show the segment-depending partitioning and state reduction for $J = 1$ and $J = 2$. The segments for $J = 1$ show four, and eight transitions per state, respectively. At this point RSSE has to consider a different amount of information in the path register for each segment.

The resulting trellis shows a less decreased minimum Euclidean distance when compared to the uniform partitioning but has a slightly higher computational complexity because of the extra states. Thus, the segment-dependent partitioning technique enables an even more flexible way to trade between complexity and performance.

V. NUMERICAL RESULTS

In this section we will give numerical simulation results and investigate several ISI-channels for *punctured* TCM. We analyse the decoder complexity as *number of branch metric calculations per information bit* and show that this approach enables a flexible trade-off between computational complexity and performance.

Due to the minimum phase characteristics of the ISI-channel the partitioning of the trellis states into hyperstates leads to the smallest possible loss in Euclidean distance. Hence, if, for instance, the ISI-channel is an equal tab delay line, the loss in Euclidean distance is higher than for an exponentially decaying channel because of the premature decisions for a surviving path.

To see this effect we conducted simulations over different ISI-channels of unit energy and plotted the complexity number over the required $\frac{E_b}{N_0}$ to achieve a bit error probability of less than 10^{-3} . The unit energy channels are defined as:

$$h_{\text{exp}}[\kappa] = \frac{1}{\sqrt{\sum_{\kappa} |h_{\text{exp}}[\kappa]|^2}} e^{(-\kappa/\kappa_0)} \quad \text{for } 0 \leq \kappa \leq L$$

$$h_{\text{lin}}[\kappa] = \frac{1}{\sqrt{\sum_{\kappa} |h_{\text{lin}}[\kappa]|^2}} \frac{L - \kappa + 1}{L + 1} \quad \text{for } 0 \leq \kappa \leq L$$

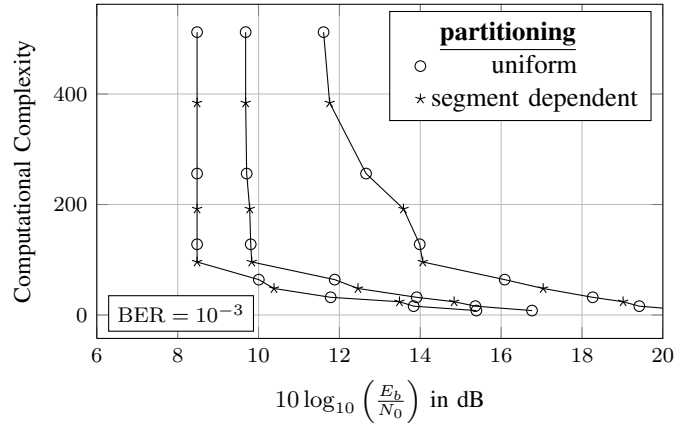


Fig. 7. Decoding complexity for a P-TCM transmission scheme with generator polynomials $[13\ 15]_{\text{oct}}$, puncturing scheme $[(11)^T\ (01)^T]$ (Rate: $\frac{4}{3}$) natural labeling and 4-ASK signaling over three different ISI-channels $h_{\text{exp}}[\kappa]$ ($\kappa_0 = 1$), $h_{\text{lin}}[\kappa]$, $h_{\text{equ}}[\kappa]$ (solid: Uniform partitioning, dashed: Segment-dependent partitioning).

$$h_{\text{equ}}[\kappa] = \frac{1}{\sqrt{\sum_{\kappa} |h_{\text{equ}}[\kappa]|^2}} = \frac{1}{\sqrt{L}} \quad \text{for } 0 \leq \kappa \leq L$$

The results can be seen in Fig. 7. As should be clear to the reader, the loss in Euclidean distance is smallest for an exponentially decaying ISI-channel.

VI. CONCLUSION

It has been shown that TCM can be extended by puncturing. Furthermore, an efficient MLSE decoder for P-TCM over ISI-channels was proposed and investigated.

The numerical simulation results clearly show that we can achieve a soft trade-off between spectral and power efficiency easier and more flexibly than by means of traditional TCM.

REFERENCES

- [1] G. Ungerboeck, "Trellis-coded modulation with redundant signal sets; part i: Introduction; part ii: State of the art," *Communications Magazine, IEEE*, vol. 25, no. 2, pp. 5–21, February 1987.
- [2] T. Hehn and J. B. Huber, "LDPC Codes and Convolutional Codes with Equal Structural Delay: A Comparison," *IEEE Transactions on Communications*, vol. 57, no. 6, pp. 1683–1692, June 2009.
- [3] E. Zehavi, "8-PSK Trellis Codes for a Rayleigh Channel," *IEEE Transactions on Communications*, vol. 40, no. 5, pp. 873–884, may 1992.
- [4] F. Schuh, A. Schenk, and J. Huber, "Reduced complexity Super-Trellis decoding for convolutionally encoded transmission over ISI-Channels," in *2013 International Conference on Computing, Networking and Communications, Signal Processing for Communications Symposium (ICNC'13 - SPC)*, San Diego, USA, Jan. 2013.
- [5] —, "Matched decoding for punctured convolutional encoded transmission over ISI-Channels," in *9th International ITG Conference on Systems, Communications and Coding 2013 (SCC'2013)*, Munich, Germany, Jan. 2013.
- [6] T. Woerz and R. Schweikert, "Performance of punctured pragmatic codes," in *Global Telecommunications Conference, 1995. GLOBECOM '95*, IEEE, vol. 1, nov 1995, pp. 664–669 vol.1.
- [7] F. Schuh, A. Schenk, and J. Huber, "Punctured Trellis-Coded Modulation," in *submitted to ICC 2014*, Jun. 2014.
- [8] M. Eyuboglu and S. Qureshi, "Reduced-State Sequence Estimation With Set Partitioning and Decision Feedback," *IEEE Trans. Commun.*, vol. 36, no. 1, pp. 13–20, Jan. 1988.
- [9] A. Duel-Hallen and C. Heegard, "Delayed Decision-Feedback Sequence Estimation," *IEEE Trans. Commun.*, vol. 37, no. 5, pp. 428–436, May 1989.
- [10] B. Spinnler and J. Huber, "Design of Hyper States for Reduced-State Sequence Estimation," in *Proc. IEEE Int. Conf. Communications ICC '95 Seattle*, vol. 1, 1995, pp. 1–6.